Lattice Defects and Oxygen Storage Capacity of Nanocrystalline Ceria and Ceria-Zirconia

E. Mamontov* and T. Egami

Department of Materials Science and Engineering, University of Pennsylvania, Philadelphia, Pennsylvania 19104-6272

R. Brezny and M. Koranne

W. R. Grace & Company−Conn. Grace Davison Research, Columbia, Maryland 21044-4098

S. Tyagi

Department of Physics, Drexel University, Philadelphia, Pennsylvania 19104

Received: June 27, 2000; In Final Form: September 19, 2000

The atomic structures of nanocrystalline powders of ceria, CeO_2, and ceria-zirconia solid solution, $(Ce,Zr)O_2$, were studied by the pulsed neutron diffraction technique. Ceria is used as an oxygen storage component in automotive exhaust emission control systems, but the degradation of its oxygen storage capacity (OSC) after extended use at high temperatures has been a problem. Our results for the first time establish a direct correlation between the concentration of vacancy-interstitial oxygen defects and OSC. The surface area, on the other hand, exhibits much less correlation with OSC. The results also show that zirconia, which is known to retard the degradation when incorporated into ceria, reduces ceria and preserves oxygen defects. It is suggested that oxygen defects are the source of OSC in ceria-based catalyst supports, and the preservation of oxygen defects is critical for the stability of OSC against thermal aging.

1. Introduction

Ceria-based oxides are widely used in automotive exhaust emission control systems as catalyst supports and oxygen promoters. Today's three-way automotive catalytic converters must efficiently oxidize carbon monoxide and hydrocarbons and at the same time reduce nitrogen oxides. A high rate of simultaneous conversion of all the pollutants can only be achieved within a narrow operating window near the stoichiometric air-to-fuel ratio. The $CO-NO_x$ conversions are strongly affected by the local oxygen partial pressure at the catalyst surface. At high oxygen partial pressures, i.e., under lean conditions, the NO_x conversions drop off precipitously, whereas at low oxygen partial pressures, i.e., under rich conditions, the CO conversions are low. The role of ceria, and more recently ceria-zirconia, is to act as an oxygen storage-and-release component to stabilize the local oxygen partial pressure at the catalyst surface even when the air-to-fuel ratio in the engine exhaust fluctuates with time.

Pure ceria, CeO_2, has a serious problem of degradation in performance with time at elevated temperatures. Traditionally, this degradation has been attributed to decrease in its surface area and in turn its oxygen storage capacity (OSC). However, recent experimental observations on pure ceria suggest that the surface area may not be the only parameter that determines the effectiveness of ceria.[1−4] Using temperature-programmed desorption (TPD) and/or steady-state CO oxidation kinetics, it has been proposed that in pure ceria "active" weakly bound oxygen species are present, which belong to the bulk rather than to the surface.[1−4] It is likely that these weakly bound oxygen species undergo fast exchange with the environment and provide OSC. Such "active" oxygen species become deactivated following a high-temperature treatment.

Recently, we have investigated the nature of these "active" oxygen species in pure ceria using pulsed neutron diffraction. Neutron diffraction is a more powerful tool for studying the oxygen positions in oxides than X-ray diffraction because of the better scattering contrast of oxygen compared to metal ions. We have shown the presence of the vacancy-interstitial (Frenkel-type) oxygen defects in CeO_2 by analyzing the pulsed neutron diffraction data both in the reciprocal space by the Rietveld refinement and in the real space by the atomic pair-distribution function (PDF) analysis.[5,6] These defects were found to disappear following a high-temperature treatment of 1073 K (800 °C). It is possible that the interstitial oxygen ions are the "active" species that provide necessary oxygen mobility crucial in the functioning of ceria as a catalyst support. We speculated that the decreasing concentration of the Frenkel-type oxygen defects at high temperatures contributes to deterioration of the oxygen storage properties in thermally aged ceria. The purpose of the present work is to establish a direct link between these defects and OSC, by carrying out the pulsed neutron diffraction measurements and the OSC measurements on similar samples after various thermal treatments.

Zirconia, ZrO_2, is known to alleviate partially the degradation of ceria at high temperatures. The beneficial effect of doping ceria with zirconia is believed to be due to stabilizing the surface area by suppressing thermal sintering.[7] However, it has been observed that ceria-zirconia mixed oxides with low surface area still maintain a high oxygen storage capacity compared to undoped ceria, and therefore other mechanisms must be present.[8] A number of recent studies have characterized the enhanced OSC of ceria-zirconia relative to ceria.[9−12] In addition, several studies have addressed the relationship between the local structure of ceria-zirconia and its OSC primarily using EXAFS

10.1021/jp0023011 CCC: $19.00
Published on Web 10/27/2000

and Raman spectroscopy.[13−15] However, the structural models analyzed in those studies included only local displacements of oxygen ions from their positions in the fluorite structure, but not the Frenkel-type oxygen defects.

In the present work it is shown that zirconia keeps ceria slightly reduced, and preserves oxygen defects up to high temperatures. We suggest that the enhanced stability of oxygen defects in ceria-zirconia accounts for the improved oxygen storage capacity and thermal stability of ceria-zirconia systems.

2. Experimental Section

2.1. Sample Preparation. The CeO_2 sample was produced by W. R. Grace & Co. by spray drying and calcining cerium acetate at 500 °C. The BET surface area of the sample was 75 m^2/g. The concentration of impurities (mostly La_2O_3) in the sample was 0.85 mol %. The $(Ce,Zr)O_2$ solid solution sample was also produced by W. R. Grace & Co. via solution decomposition technique from mixed acetate solutions. Solutions of cerium acetate and zirconium acetate were mixed together to give the desired composition. The homogeneously mixed solutions were spray dried at 150 °C to give a fine mixed acetate powder. The powder was calcined at 500 °C to form the mixed oxide. The BET surface area of the sample was 26 m^2/g. The sample composition was 67 mol % of CeO_2, 30.5 mol % of ZrO_2, and 2.5 mol % of rare-earth oxide impurities (mostly La_2O_3).

2.2. Neutron Diffraction and Data Analysis. Neutron diffraction experiments were carried out at the Special Environment Powder Diffractometer at the Intense Pulsed Neutron Source (IPNS) of Argonne National Laboratory using the time-of-flight method. Prior to the experiment the samples were outgassed by heating to 300 °C in the sample chamber for 4 h. For ceria as well as ceria-zirconia samples diffraction data were collected at room temperature for 4 h. Then the temperature was progressively raised according to the following regimen. A target temperature was chosen, and the samples were heated to this temperature at the rate of 3 °C/min. After 15−20 min allowed for thermal equilibration the diffraction data were collected for approximately 4 h. Then the next target temperature was chosen, and so on. After collecting diffraction data at the highest temperature, the samples were cooled to room temperature over an 8 h time-period and then diffraction data were collected again for approximately 3 h at room temperature. In the course of the measurements and the thermal treatment, the vacuum in the sample chamber was $\sim 10^{-6}$ Torr.

The diffraction data collected at the high-resolution detector bank ($\Delta d/d = 0.0054$, $2\theta = 90°$) were analyzed by the Rietveld method using the IPNS Rietveld package[16] over the d range of 0.5−3.6 Å. The refinement of structural parameters in the Rietveld analysis is achieved by means of least-squares fitting of the diffraction data with the model diffraction pattern. As a measure of goodness of the fit we used the Rietveld refined weighted profile reliability factor R_w defined in the usual manner.[16] The scattering lengths used in the Rietveld analysis were 0.484×10^{-12} cm for cerium, 0.716×10^{-12} cm for zirconium, and 0.580×10^{-12} cm for oxygen. The background was modeled using a polynomial function and was subtracted from the diffraction pattern. The peak profile was modeled using a two-sided exponential function that was convoluted with a Gaussian function to describe the instrumental and sample contributions, respectively. The overall scale factor, background parameters, unit cell parameter, peak shape parameters, and isotropic thermal factors were refined. Attempts to refine other parameters, such as extinction and absorption coefficients, diffractometer constants, and counter-zero error, resulted in no appreciable improvement of agreement with the experiment. The anharmonic thermal factors for oxygen atoms were tried, but also did not improve the agreement with the experiment.

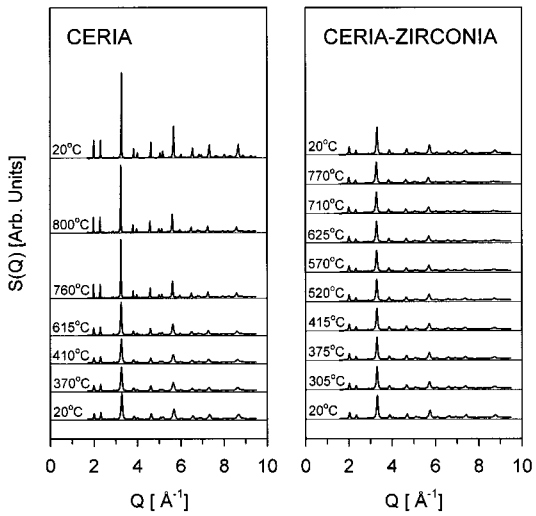

Figure 1. Temperature dependence of the neutron diffraction patterns.

2.3. Temperature-Programmed Reduction Measurements. The temperature-programmed reduction (TPR) measurements were carried out by flowing 5% CO in He over 500-mg samples. The sample temperature was raised at the rate of 20 °C/min up to 1000 °C. The output CO_2 signal was continuously monitored using a mass spectrometer. The TPR measurements for ceria-zirconia were performed on the as prepared sample and the sample aged at 850 °C for 5 h in air in a muffle furnace. For ceria, the TPR measurements were performed on the as prepared sample and those aged for 5 h at 700 °C, 750 °C, and 800 °C in air in a muffle furnace. The oxygen storage capacity was calculated from the TPR profiles and defined as the amount of reducible oxygen up to a temperature of 700 °C. This temperature was selected so as to capture the information from the low-temperature CO_2 output peak.

2.4. Electron Paramagnetic Resonance Measurements. The electron paramagnetic resonance (EPR) measurements were performed using an X-band Varian E−12 EPR spectrometer with a rectangular T_{102} microwave cavity. The spectra were calibrated with a diphenylpicrylhydrazyl (DPPH) standard ($g = 2.0036$). The measurements carried out at room temperature and at 77 K showed no appreciable difference in line positions.

3. Results

3.1. Neutron Diffraction and Rietveld Refinement. The temperature dependence of the neutron diffraction patterns for ceria and ceria-zirconia solid solution is shown in Figure 1. The data are presented as a function of the scattering vector Q, defined as $Q = |\mathbf{Q}| = 4\pi\sin\theta/\lambda$ and calculated from the neutron time-of-flight. The diffraction pattern for ceria exhibits peak shape change with increasing temperature due to crystallite size growth. On the other hand, the peak shape for ceria-zirconia remains virtually unchanged with increasing temperature indicating that the crystallite growth in ceria-zirconia is negligible even after a thermal treatment of 770 °C. As one can see in Figure 2, the crystallite size determined by the peak width ($=2\pi$/FWHM) is approximately 80 Å in both samples as prepared, and for ceria after the thermal treatment it grows appreciably, while little growth is observed for ceria-zirconia. These results are consistent with previous studies on suppression of crystallite

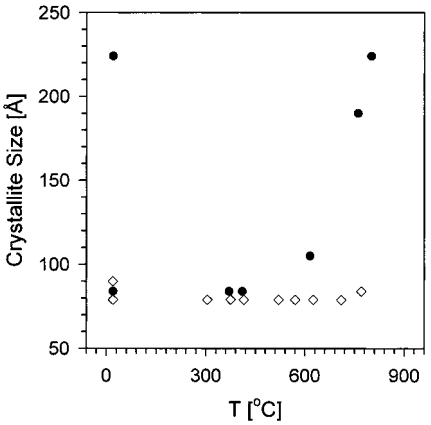

Figure 2. Temperature dependence of the crystallite size in ceria (filled circles) and ceria-zirconia (open diamonds). At 20 °C the larger crystallite sizes correspond to the data collected after the completion of the thermal cycles.

growth by doping ceria with zirconia. It is important to note that there are no extra peaks in the ceria-zirconia diffraction pattern compared to that for CeO_2, and the peak profiles could be satisfactorily fitted with a single Gaussian. This suggests that in our sample ceria and zirconia form a cubic single-phase solid solution. For samples of nominal 70 mol % ceria and 30 mol % zirconia composition, the formation of a cubic single-phase solid solution was observed previously by X-ray diffraction.[9]

Ceria and cubic ceria-zirconia solid solutions possess a fluorite structure, which is presented in Figure 3a. It can be viewed as an array of oxygen ions forming a simple cubic lattice where cations occupy the centers of each second oxygen cube. Alternatively, it can be described as an array of cations forming the face-centered-cubic lattice with oxygen ions occupying the tetrahedral interstitial sites. The octahedral sites in a perfect fluorite structure are empty. In our previous study we have demonstrated that in ceria, like in many other fluorites, some anions may relocate themselves from the tetrahedral sites to the octahedral sites, leaving vacancies in the tetrahedral sites and resulting in the formation of the Frenkel-type anion defects.[6] It was found that structural models such as the one shown in Figure 3b that incorporated oxygen interstitial ions in octahedral sites and vacancies in tetrahedral sites yielded the best fit for the diffraction data on pure ceria.[6] Hence, in the Rietveld refinement for ceria and ceria-zirconia reported here, we used the structural model shown in Figure 3b. The small relaxation displacements of the oxygen ions in the tetrahedral sites next to the Frenkel-type defects were previously found to produce no appreciable improvement in the Rietveld refinement, even though they were important to the pair-distribution function analysis, and thus were not considered in the present work.

In the Rietveld refinement reported in this work we did not assume oxygen stoichiometry either for ceria or for ceria-zirconia. Instead, the concentrations of oxygen interstitial ions and vacancies were refined independently. For clarity, the refinement procedure is illustrated in Figure 4 using the data on the ceria-zirconia prior to the thermal treatment as an example. First, the concentration of vacancies was refined, assuming there were no interstitial oxygen ions. A minimum in the agreement factor at a vacancy concentration of 17% was obtained as seen in Figure 4a. Holding the vacancy concentration at 17%, the concentration of interstitial oxygen was refined and a minimum in the agreement factor was obtained at an interstitial concentration of 9%. The results were found to be independent of the order of refinement, as shown in Figure 4b, where the concentration of the interstitial ions was refined first followed

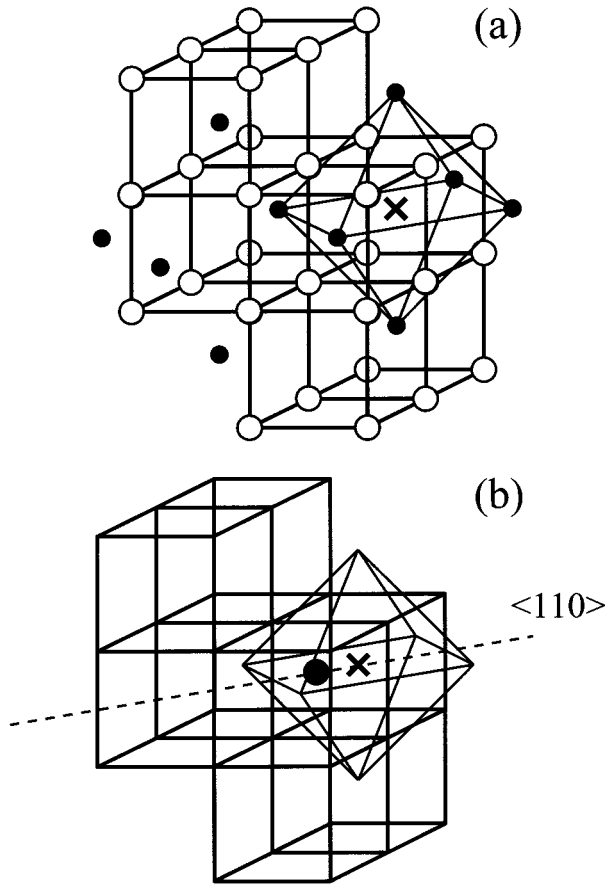

Figure 3. The structure of ceria and cubic ceria-zirconia solid solution. (a) Perfect fluorite structure. Cations (small filled circles) occupy each second interstitial site of the cubes of oxygen ions (open circles). Cation sublattice forms tetrahedral and octahedral sites (one of the octahedral sites is shown). The centers of the tetrahedral sites coincide with the vertexes of the oxygen cubes, while those of the octahedral sites (marked by a cross) coincide with the centers of the oxygen cubes. All the tetrahedral sites are filled by oxygen ions, and all the octahedral sites are empty. (b) Oxygen defects in fluorite structure. Some oxygen ions (filled circle) occupy the interstitial octahedral sites, leaving vacancies in the tetrahedral sites (not shown). The interstitial oxygen ions are displaced from the centers of the interstitial octahedral sites in the ⟨110⟩ directions. In the general case, the concentration of vacancies may exceed that of interstitial ions, resulting in oxygen nonstoichiometry.

by the refinement of the concentration of vacancies. If we tried to refine the concentrations of interstitial ions and vacancies at the same time, the refinement diverged. The procedure above to refine each parameter one at a time also has the benefit of being able to determine the magnitude of errors. The boxes near the minima in Figure 4 show the errors in the refined values of concentration at 90% significance level estimated according to the Hamilton's significance test.[17] In this particular refinement, with 90% confidence the concentration of interstitial oxygen ions falls within the limits of 7% to 14%, and that of vacancies is between 15% and 22%. In summary, for the ceria-zirconia sample prior to the thermal treatment the concentration of vacancies and interstitial ions were determined to be 17% and 9%, respectively. Similar refinement procedure was performed for all sets of the diffraction data shown in Figure 1, and the results on the oxygen defect concentration were plotted in Figure 5, where filled circles represent interstitial ions, and open circles stand for vacancies. At room temperature there are two sets of data for both ceria and ceria-zirconia; the lower concentrations

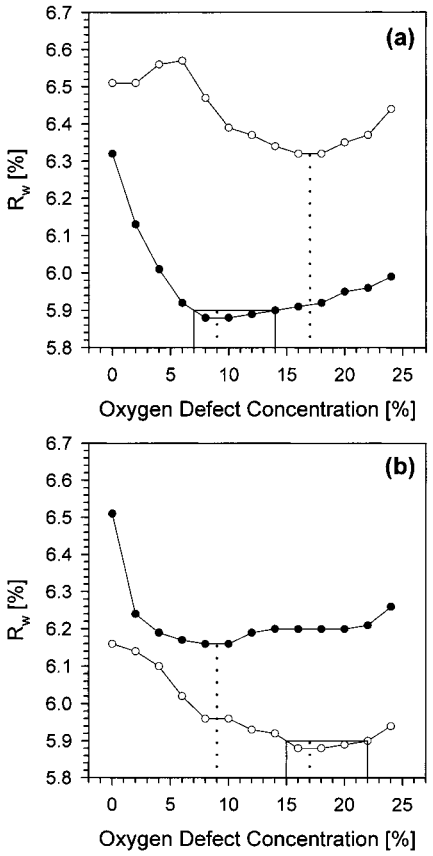

Figure 4. The illustration of the structural refinement procedure using the data on ceria-zirconia prior to the thermal treatment as an example. (a) The concentration of vacancies is refined first (open circles) assuming no interstitial ions, and the minimum at 17% (dotted line) is found. Then the concentration of interstitial ions is refined (filled circles) holding the concentration of vacancies at 17%, and the minimum at 9% (dotted line) is found. (b) The concentration of interstitial ions is refined first (filled circles) assuming no vacancies, and the minimum at 9% (dotted line) is found. Then the concentration of vacancies is refined (open circles) holding the concentration of interstitial ions at 9%, and the minimum at 17% (dotted line) is found. The results are independent of the order of the refinement procedure. The boxes near the minima show the errors in the refined values of concentrations at 90% significance level estimated according to the Hamilton's significance test.[17]

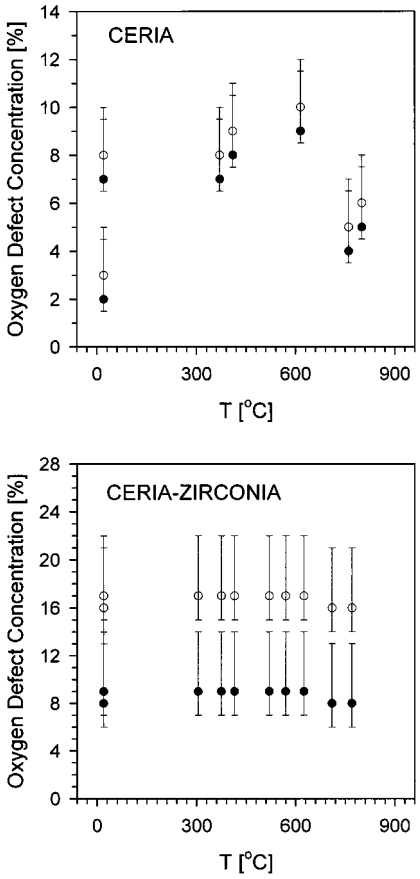

Figure 5. Temperature dependence of the oxygen defect concentration. Filled circles: oxygen interstitial ions, open circles: oxygen vacancies. Errors are estimated as shown in Figure 4. At 20 °C there are two sets of data for both ceria and ceria-zirconia; the lower concentrations of vacancies and interstitial ions correspond to the data collected after the completion of the thermal cycles.

of vacancies and interstitial ions in Figure 5 correspond to the data collected after the completion of the thermal cycles.

As can be seen from Figure 5, the concentration of oxygen defects and its temperature dependence differ dramatically for ceria and ceria-zirconia. In ceria, the total oxygen composition of the sample remains close to stoichiometric, that is, CeO_2, through the thermal treatment cycle, as indicated by the fact that the vacancy and the interstitial ion concentrations remain equal within the limits of the error. In ceria-zirconia, however, the difference between the concentration of vacancies and interstitial ions is as much as 8%. Such a substantial difference exceeds the limits of the error and only in part can be attributed to trivalent impurities such as La^{3+}. Even if we assume that all the impurities in the ceria-zirconia sample (∼2.5%) are trivalent, it accounts only for 1.25% of vacancies. This indicates that the ceria-zirconia sample is oxygen-deficient, and remains so through the thermal treatment process. While in the ceria-zirconia sample both vacancy and interstitial defect concentrations remain virtually unchanged in the course of the thermal cycling, in the undoped ceria they fall at 760 °C, and after the completion of the thermal cycle only a small fraction of the Frenkel-type defects is retained. In agreement with our previous

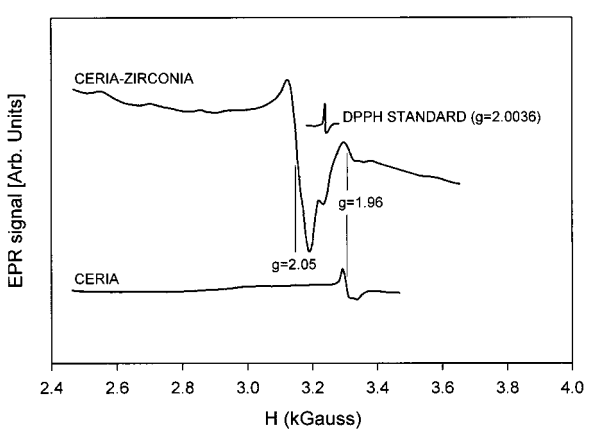

Figure 6. The EPR spectra obtained from the as prepared samples at 77 K. The DPPH calibration spectrum ($g = 2.0036$) is included.

results,[6] this indicates that irreversible recombination of interstitial oxygen ions with vacancies takes place in ceria at temperatures around 760 °C.

3.2. Electron Paramagnetic Resonance. The EPR spectra obtained from the as prepared samples at 77 K are presented in Figure 6 along with the DPPH calibration spectrum. The ceria as well as ceria-zirconia spectra show a line at $g = 1.96$, which has been assigned previously to impurity-related defects.[18−20] The absence of other lines in the ceria spectrum suggests that the interstitial oxygen ions in octahedral sites are in the O^{2-} state, and the corresponding vacancies constituting the Frenkel-

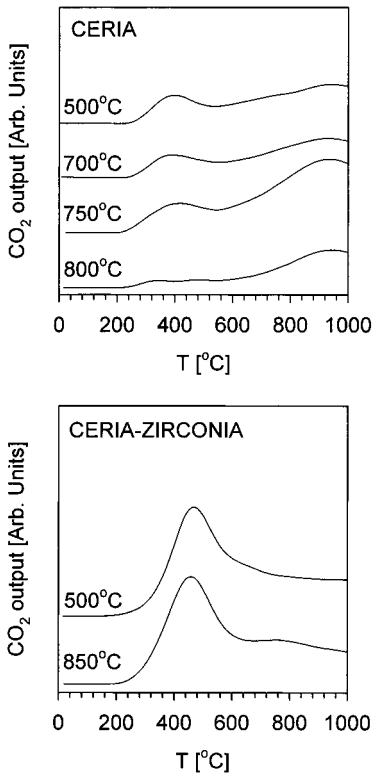

Figure 7. CO_2 output profiles in the temperature-programmed reduction experiment using CO. Sample aging temperatures are shown next to the TPR profiles.

type defects do not have any trapped electrons. Thus, neither vacancies nor interstitial ions contribute to EPR. In such a scenario, annihilation of the Frenkel-type defects would not affect the EPR signal. This was confirmed by EPR measurements on the ceria sample aged at 800 °C, wherein the EPR spectrum (not shown in Figure 6) remained unchanged.

In addition to the line at $g = 1.96$, the ceria-zirconia sample exhibits a strong resonance line, the fine structure of which is poorly resolved. The main feature of this line corresponds to $g = 2.05$. The EPR spectrum of the ceria-zirconia sample aged at 850 °C (not shown in Figure 6) also exhibits this strong resonance line at $g = 2.05$. Since Zr^{4+} cations do not contribute to EPR, this strong line is probably due to the presence of Ce^{3+} ions and corresponding oxygen vacancies. Such vacancies may trap electrons that give rise to the paramagnetic signal, in contrast to vacancies originated from mere relocation of O^{2-} ions as described above. Besides, Ce^{3+} ions themselves may contribute to the resonance line at $g = 2.05$. The $4f^1$ electrons localized on Ce^{3+} sites are often subjected to spin−lattice relaxation processes that will broaden their EPR lines beyond detection except for measurements at very low temperatures.[21] However, a very asymmetric environment such as in the case of Ce^{3+} ions associated with an oxygen vacancy can quench spin−lattice relaxation to some extent and result in a detectable EPR signal.[22] In any case, a strong extra line in the ceria-zirconia EPR spectrum shows that its electronic structure is substantially different from that of the undoped ceria. This is what one would expect in the presence of extra oxygen vacancies in oxygen-deficient ceria-zirconia.

3.3. Temperature-Programmed Reduction. Figure 7 shows the temperature-programmed reduction (TPR) profiles for fresh and aged ceria as well as ceria-zirconia samples. As one can see, ceria exhibits a broad reduction profile with a low-temperature CO_2 peak centered around 400 °C and a high-temperature CO_2 peak centered around 900 °C. The area under the low-temperature peak is of particular interest since it relates to the low-temperature oxygen storage capacity of this material. The oxygen contributing to the low-temperature CO_2 peak is the most readily available during automotive converter operation. The oxygen storage capacity measured up to 700 °C is summarized in Table 1 along with the surface area of the samples. It is interesting to note that the area under the low-temperature CO_2 peak is fairly constant up to an aging temperature of 750 °C but decreases dramatically when the sample is aged at 800 °C.

TABLE 1: Oxygen Storage Capacity and the Surface Area of the Samples

sample	aging temperature, °C	OSC measured in CO TPR up to 700 °C, μmoles O_2/g	surface area, m^2/g
ceria	500	186	75
	700	186	50
	750	217	38
	800	62	37
ceria-zirconia	500	543	26
	850	558	10

In contrast to the TPR profiles for ceria, the ceria-zirconia reduction profiles exhibit a single reduction peak centered at 460 °C. Such a single reduction peak is indeed characteristic of ceria-zirconia and is in agreement with other TPR measurements performed using hydrogen as a reductant.[10,11] More importantly, the area under this peak does not decrease even after aging the ceria-zirconia sample at 850 °C. This is one of the primary reasons why ceria-zirconia has virtually replaced all ceria in modern automotive catalytic converters.

4. Discussion

The results of our studies clearly demonstrate the presence of oxygen vacancies and interstitial ions in pure ceria nanocrystals and in a nano-crystalline solid solution of ceria and zirconia. In materials with a fluorite structure Frenkel-type anion defects have been observed in both doped compounds, where the interstitial anions are charge-compensated,[23−25] and in pure tetravalent systems.[26] In the latter case interstitial anions are charge-compensated by vacancies in the regular anion sublattice. In the Rietveld refinement performed in this work the oxygen stoichiometry was not assumed. For ceria, the concentrations of the interstitial ions and vacancies turned out to be equal. Along with the absence of EPR active oxygen species, such as O_2^{2-} or O^-, this suggests that the interstitial oxygen ions exist as O^{2-} species and are charge-compensated by corresponding vacancies. For ceria-zirconia, however, the Rietveld analysis shows that the concentration of vacancies far exceeds that of interstitial ions, indicating substantial oxygen deficiency. Thus, in addition to vacancies originating from mere relocation of oxygen ions into the octahedral interstitial sites, there are some excessive vacancies that require the presence of $Ce^{3+}(4f^1)$ cations in order to maintain electrical neutrality. The difference between the EPR spectra of undoped ceria and ceria-zirconia that we observed is in agreement with this interpretation.

The substantial oxygen deficiency observed in the ceria-zirconia sample (7−8%) is particularly fascinating considering the similarity of processing applied to both the ceria and the ceria-zirconia sample. We believe this is an intrinsic property of a ceria-zirconia solid solution, and must be related to the relative instability of Ce^{4+} ions which makes ceria an attractive material for oxygen storage to begin with. It was suggested

previously that doping ceria with zirconia may promote formation of Ce^{3+} ions due to the smaller size of Zr^{4+} cations that take part in removing the strain associated with the increase of ionic size accompanying the $Ce^{4+} \rightarrow Ce^{3+}$ transition.[27]

The difference in the temperature dependence of defect concentration in ceria and ceria-zirconia is quite striking. While ceria exhibits a dramatic drop in the concentrations of vacancies and interstitial ions following high temperature treatment, these concentrations remain virtually constant in ceria-zirconia. As we suggested previously,[6] the interstitial oxygen ions in ceria-containing compounds are likely to form during sample processing. When oxygen-deficient material is oxidized to CeO_2 or $(Ce,Zr)O_2$, absorbed oxygen ions may at first enter the roomier octahedral sites, rather than fill the spatially tight tetrahedral sites. If annealing temperature is not high enough they may not be able to overcome a potential barrier to get into the regular tetrahedral sites, and remain in the octahedral sites. Only when the sample is treated at sufficiently high temperature thermally activated interstitial ions may enter regular tetrahedral sites and recombine with vacancies. Because of the smaller ionic radius of zirconium ions, mixing zirconia with ceria will reduce the lattice constant and produce the atomic-level pressure[28] at the smaller tetrahedral sites, making them even more difficult to reach for the interstitial oxygen ions than in pure ceria. This may explain the enhanced stability of oxygen defects against thermal aging in ceria-zirconia, where the recombination of interstitial ions with vacancies may be expected to occur at higher temperatures compared to pure ceria. To this end, interesting results obtained by EXAFS were reported recently.[15] These results suggested a difference in the local oxygen environment of cerium and zirconium cations in two compositionally similar $Ce_{0.6}Zr_{0.4}O_2$ samples, the synthesis procedures for which were different and involved thermal treatments at 773 K for one (high-surface-area) sample and at 1873 K for the other (low-surface-area) sample. Not only the cation−anion coordination numbers were different between the two samples, but also the Debye−Waller factors for the high-surface-area sample were substantially lower, indicating less disorder in the oxygen sublattice. The authors proposed that the increase in the treatment temperature must have induced some structural rearrangements in the lattice, though the nature of the rearrangements was not discussed. We believe that these EXAFS results may be indicative of the changes in the oxygen sublattice that occur in ceria-zirconia treated at 1873 K due to recombination of interstitial oxygen ions with vacancies, but not in ceria-zirconia treated at 773 K.

In our earlier work[6] we had suggested that the interstitial oxygen ions are the "active" ions that provide necessary mobility crucial to the function of ceria as an oxygen storage medium. In addition we proposed that apart from decreasing surface area the annihilation of the oxygen Frenkel-type defects might contribute to deterioration of the oxygen storage capacity in thermally aged automotive catalyst supports. The data presented in Table 1 clearly indicate that diminishing oxygen storage capacity in the aged ceria samples we studied cannot be due to changes of surface area alone. The OSC falls sharply between the aging temperatures of 750 °C and 800 °C. It is noteworthy that this drop is not accompanied by a comparable decrease in the surface area, which decreases gradually with temperature. Similarly, the crystallite size increases by about 25% when annealed at 615 °C, and continuously grows with increasing temperature (see Figure 2). In contrast, the concentration of oxygen defects and the amount of "active" oxygen remain unchanged up to higher temperatures (see Figure 5 and Table 1). Instead of gradual changing with increasing temperature as observed for the surface area and crystallite size, they both drop dramatically at 760−800 °C. This observation suggests the correlation between oxygen defect concentration and oxygen storage capacity.

For ceria-zirconia, the aging at 850 °C does not affect the amount of "active" oxygen appreciably despite a substantial decrease of the surface area (see Table 1). It is also interesting to note that the OSC of ceria-zirconia is much higher despite significantly lower surface area, not only for aged samples but also for the samples as prepared. These observations drive us to the conclusion that the activity of the ceria and the ceria-zirconia samples as oxygen storage media does not correlate with surface area alone. On the other hand, the dependence of this activity on the aging temperature resembles the temperature dependence of the oxygen defect concentration shown in Figure 5, which falls sharply at 760 °C in the ceria sample and remains unchanged in the ceria-zirconia sample. Therefore, while surface area is undoubtedly an important parameter affecting the oxygen storage properties in ceria-containing oxides, the presence of oxygen defects in these materials may be a prerequisite for their catalytic activity at moderate temperatures.

The detailed mechanism of how the oxygen defects ensure the catalytic activity of ceria-containing oxides requires further exploration. While previously we suggested that the interstitial oxygen ions may themselves play a role of "active", weakly bound oxygen species, it is also possible that the presence of oxygen vacancies is crucial to the function of oxygen storage media. In this case the role of oxygen interstitial ions may be to create and maintain vacancies in the oxygen sublattice. We propose that ceria-containing oxides with low concentrations of both oxygen vacancies and interstitial ions are not catalytically active at moderate temperatures. Presently it is not clear whether interstitial ions or vacancies are the most important for oxygen storage capacity. Further experiments aimed at answering this question are currently underway.

Finally, we suggest that doping ceria with zirconia may improve the oxygen storage properties of ceria at three different levels. At the level of the microstructure, it inhibits surface diffusion and in turn the loss of surface area at high temperatures. At the mesoscopic level, substantial doping may result in the formation of an interface structure that facilitates the oxygen transport from bulk to the surface.[8,29,30] Besides, as demonstrated by the current study, at the atomic-level, it stabilizes the oxygen defective structure. We believe that probing ceria-zirconia system using neutron scattering has elucidated the importance of oxygen defective structure to the function of oxygen storage catalysts.

5. Conclusion

We studied the atomic-level defective structure of nanoscale powders of ceria and ceria-zirconia solid solution using the pulsed neutron diffraction technique. The samples as prepared contained substantial amount of oxygen defects consisting of the oxygen interstitial ions in the octahedral sites and the oxygen vacancies in the tetrahedral sites of the cation sublattice. In ceria, the concentration of vacancies was close to the concentration of interstitial ions, so the total oxygen stoichiometry was maintained. In ceria-zirconia, we observed substantially more vacancies than interstitial ions, and the net oxygen deficiency totaled 8%. Such a large oxygen deficiency cannot be explained by the presence of trivalent impurities, and must be an intrinsic property of ceria-zirconia solid solutions. It is possible that in mixed ceria-zirconia oxides a smaller ionic radius of zirconium

favors the presence of Ce^{3+} ions by eliminating the strain associated with their formation. The suggested presence of Ce^{3+} ions and associated oxygen vacancies in the ceria-zirconia sample was in agreement with the results of EPR measurements. The temperature-dependent behavior of the oxygen defective structure differed dramatically between ceria and ceria-zirconia. In the former, the Frenkel-type defects annihilated at high temperature due to recombination of the interstitial ions with the vacancies, and after the completion of the thermal cycle only a small fraction of the defects was retained. In the latter, the concentrations of both oxygen vacancies and interstitial ions remained unchanged in the course of similar thermal treatment. We speculate that because of the local atomic compressive stresses at the spatially tight tetrahedral sites in the ceria-zirconia caused by a smaller ionic radius of zirconium it is more difficult for the interstitial oxygen ions to reach the tetrahedral sites and recombine with vacancies. Very importantly, the dependence of the amount of weakly bound, catalytically active oxygen in CeO_2 on the aging temperature determined in the CO TPR experiment correlated with the temperature dependence of the oxygen defect concentration, and showed poor correlation with surface area. We propose that oxygen defects in ceria-containing materials may be a prerequisite for their catalytic activity at moderate temperatures. We suggest that the enhanced stability of oxygen defects may account for the improved oxygen storage capacity and thermal stability of ceria-zirconia systems compared to pure ceria. In addition to previously known micro- and mesoscopic scale effects, this mechanism acting at the atomic-scale level must be important to the function of ceria-zirconia mixed oxides in automotive three-way catalytic converters.

Acknowledgment. The authors are grateful to M. Juskelis for assistance with the TPR measurements. They are also thankful to S. Short and J. Mitchell for technical assistance. The research was supported by the U.S. Department of Energy and the National Science Foundation through the Automotive Initiative Grant DE-FG02-96ER14682.A000. This work has benefited from the use of the Intense Pulsed Neutron Source at Argonne National Laboratory which is funded by the U.S. Department of Energy, BES-Materials Science, under Contract W-31-109-ENG-38.

References and Notes

(1) Putna, E. S.; Vohs, J. M.; Gorte, R. J. *J. Phys. Chem.* **1996**, *100*, 17862.
(2) Putna, E. S.; Vohs, J. M.; Gorte, R. J. *Catal. Lett.* **1997**, *45*, 143.
(3) Cordatos, H.; Bunluesin, T.; Stubenrauch, J.; Vohs, J. M.; Gorte, R. J. *J. Phys. Chem.* **1996**, *100*, 785.
(4) Bunluesin, T.; Gorte, R. J.; Graham, G. W. *Appl. Catal. B* **1997**, *14*, 105.
(5) Mamontov, E.; Egami, T.; Brezny, R. In *Advanced Catalytic Materials-1998*; Lednor, P. W., Nagaki, D. A., Thompson, L. T., Eds.; Materials Research Society: Boston, MA, 1998; Vol. 549, p 185.
(6) Mamontov, E.; Egami, T. *J. Phys. Chem. Solids* **2000**, *61*, 1345.
(7) Ozawa, M.; Kimura, M.; Isogai, A. *J. Alloys Compd.* **1993**, *193*, 73.
(8) Egami, T.; Dmowski, W.; Brezny, R. *SAE J.* **1997**, Paper No. 970461.
(9) Fornasiero, P.; Di Monte, R.; Ranga Rao, G.; Kaspar, J.; Meriani, S.; Trovarelli, A.; Graziani, M. *J. Catal.* **1995**, *151*, 168.
(10) Fornasiero, P.; Balducci, G.; Di Monte, R.; Kaspar, J.; Sergo, V.; Gubitosa, G.; Ferrero, A.; Graziani, M. *J. Catal.* **1996**, *164*, 173.
(11) Vidmar, P.; Fornasiero, P.; Kaspar, J.; Gubitosa, G.; Graziani, M. *J. Catal.* **1997**, *171*, 160.
(12) Fornasiero, P.; Kaspar, J.; Sergo, V.; Graziani, M. *J. Catal.* **1999**, *182*, 56.
(13) Vlaic, G.; Fornasiero, P.; Geremia, S.; Kaspar, J.; Graziani, M. *J. Catal.* **1997**, *168*, 386.
(14) Vlaic, G.; Di Monte, R.; Fornasiero, P.; Fonda, E.; Kaspar, J.; Graziani, M. *J. Catal.* **1999**, *182*, 378.
(15) Fornasiero, P.; Fonda, E.; Di Monte, R.; Vlaic, G.; Kaspar, J.; Graziani, M. *J. Catal.* **1999**, *187*, 177.
(16) Von Dreele, R. B.; Jorgensen, J. D.; Windsor, C. G. *J. Appl. Crystallogr.* **1982**, *15*, 581.
(17) Hamilton W. C. *Acta Crystallogr.* **1965**, *18*, 502.
(18) Steinberg, M. *Isr. J. Chem.* **1970**, *8*, 877.
(19) Che, M.; Kibblewhite, J. F. J.; Tench, A. J.; Dufaux, M.; Naccache, C. *J. Chem. Soc., Faraday Trans.* **1973**, *69*, 857.
(20) Soria, J.; Coronado, J. M.; Conesa J. C. *J. Chem. Soc., Faraday Trans.* **1996**, *92*, 1619.
(21) Wertz, J. E.; Bolton, J. R. *Electron Spin Resonance*; McGraw-Hill: New York, 1972; p 339.
(22) Soria, J.; Martinez-Arias, A.; Conesa, J. C. *J. Chem. Soc., Faraday Trans.* **1995**, *91*, 1669.
(23) Cheetham, A. K.; Fender, B. E. F.; Cooper, M. J. *J. Phys. C: Solid State. Phys.* **1971**, *4*, 3107.
(24) Steele, D.; Childs, P. E.; Fender, B. E. F. *J. Phys. C: Solid State Phys.* **1972**, *5*, 2677.
(25) Andersen, N. H.; Clausen, K. N.; Kjems, J. K.; Schoonman, J. *J. Phys. C: Solid State. Phys.* **1986**, *19*, 2377.
(26) Hutchings, M. T.; Clausen, K.; Dickens, M. H.; Hayes, W.; Kjems, J. K.; Schnabel, P. G.; Smith, C. *J. Phys. C: Solid State Phys.* **1984**, *17*, 3903.
(27) Balducci, G.; Kaspar, J.; Fornasiero, P.; Graziani, M.; Saiful Islam, M.; Gale, J. D. *J. Phys. Chem. B* **1997**, *101*, 1750.
(28) Egami, T.; Maeda, K.; Vitek, V. *Philos. Mag. A* **1980**, *41*, 883.
(29) Dmowski, W.; Louca, D.; Egami, T.; Brezny, R. *Ceram. Trans.* **1997**, *73*, 119.
(30) Dmowski, W.; Mamontov, E.; Egami, T.; Putna, S.; Gorte, R. *Phys. B* **1998**, *248*, 95.
(31) *Corresponding author. E-mail: mamontov@seas.upenn.edu. Phone: (215) 898-7944. FAX: (215) 573-2128.